MARTENSITE TRANSFORMATION OF A TINICU ALLOY[®]

Zhang, Yi Jin, Jialing Ji, Zhiqiang Shanghai Iron and Steel Research Institute, Shanghai 200940

ABSTRACT The two-stage martensitic transformation B2-B19-B19' in a Ti49Ni41Cu10 alloy has been investigated by means of electrical resistivity, differential scanning calorimetry (DSC), elastic modulus, X-ray diffraction and TEM observation. The cubic B2-orthorhomic B19 transformation has significant transformation heat effect with clear and sharp DSC peaks in a narrow temperature range and is accompanied with a pronounced softening of the elastic modulus; but its resistivity change is minor. The orthorhomic B19-monoclinic B19' transformation has small heat effect with diffuse DSC peaks over a wide temperature range and an obvious resistivity change. TEM observation reveals the twin substructure of B19' martensite, contrasting to the defect-free B19 martensite. The difference in transformation behaviour of the B2-B19 and the B19-B19' might be related to the different martensite lattice type and substructure. The comparison between ternary and binary alloys have been also discussed.

Key words: TiNiCu shape memory alloy two-stage martensitic transformation

1 INTRODUCTION

Binary NiTi alloys exhibit excellent shape memory effect (SME). Their transformation temperatures are very sensitive to the chemical composition and treatment process of the alloy. But the transformation temperature hysteresis^[1] is slightly influenced by these factors. With increasing engineering applications, alloys with small transformation hysteresis and large recoverable strain are required. Although the B2-R transformation in NiTi alloy has only 1~2 K hysteresis, it has also too small recoverable strain (<1%) to suite the requirments. Ternary TiNiCu alloys, where some Ni of binary alloy were replaced by Cu, have minor hysteresis and adequate recoverable strain, therefore they have become one of the interesting research subjects since last decant years.

TiNiCu alloys remain homogeneous B2 parent and still appear SME in a wide composition range (up to 30 at. - % Cu content)^[2-4]. It has been found that for ternary and binary alloys the martensitic transformation characteristics represented by electrical resistivity-

temperature (R-T) curve and DSC curve are different. It is necessary to study the transformation of a TiNiCu alloy in detail. The purpose of present work is to investigate the martensitic transformation of a Ti49Ni41Cu10 alloy and compare it with that of a Ni51Ti49 alloy.

2 MATERIAL AND EXPERIMEN-TAL PROCEDURE

The alloy used in the work was multiple melted by vacuum noncosumable electrode from raw materials sponges Ti, 99. 99% Ni and 99. 99% Cu. The nominal composition of the alloy was(at.-%): 49. 0 Ti-41. 0 Ni-10. 0 Cu. The obtained circular ingot was forged isothermally and hot rolled. The specimens were heat treated at 1123 K for 0.5 h followed by air cooling.

The measurements of electrical resistivity were carried out on a SMT-1 synthetical instrument^[5]. A Dupont 2100 differential scanning calorimetry was also used to determine transformation temperatures. The flexural resonant-bar technique was used to measure

① Received June 4, 1994

the elastic modulus vs temperature. X-ray diffraction and TEM were used to analyse the microstructure.

3 RESULTS

3. 1 Electrical Resistivity-Temperature (R-T) curve

Fig. 1 shows the R-T curve of Ni51Ti49 alloy. On cooling the resistivity increases with the occurrence of B2-R transformation at T= $T_{\rm R}$ temperature and decreases with martensitic transformation from start temperature M_s until finish temperature $M_{\rm f}$. The reverse transformatin takes place on heating [6]. The R-T curve of the ternary Ti49Ni41Cu10 alloy is shown in Fig. 2, where two transformation peaks have been noticed. The first at the higher temperture has a small resistivity change and a narrow temperature range. The second at the lower temperature takes place over a wide temperature range and has a pronounced resistivity change. In this work the temperature decreases to 153 K, but this transformation is still not complete.

Using the symbols M_s' , M_f' , A_s' , A_f' and M_s , M_f , A_s , A_f to describe the start and finish temperatures of the toward and reverse transformation for the first and second one, respectively. From Fig. 2 they are determined

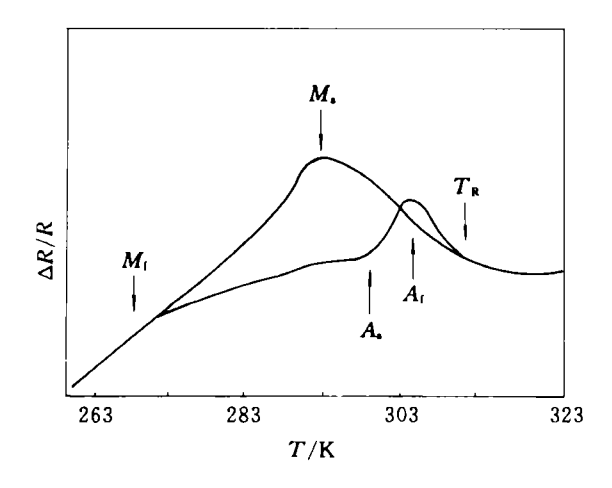


Fig. 1 R-T curve of Ni51Ti49 alloy

as the follows: $M_{\rm s}' = 308 \, {\rm K}$, $M_{\rm f}' = 301 \, {\rm K}$, $A_{\rm s}' = 303 \, {\rm K}$, $A_{\rm f}' = 315 \, {\rm K}$, $M_{\rm s} = 291 \, {\rm K}$, $M_{\rm f} < 153 \, {\rm K}$, $A_{\rm s} = 189 \, {\rm K}$, $A_{\rm f} = 293 \, {\rm K}$.

3. 2 DSC Curve

Fig. 3 shows the DSC curve of the Ti49Ni41Cu10 alloy. Two peaks can be observed on each cooling heating curves. The first peak appearing at higher temperature is clear and sharp in a narrow temperature range, from which the characteristic parameters are determined as the follows: $M_{\rm s}'=301$. $5\,{\rm K}$, $M_{\rm max}'=294$. $3\,{\rm K}$, $A_{\rm s}'=305$. $2\,{\rm K}$, $A_{\rm max}'=310$. $1\,{\rm K}$, transformation heat $\Delta H1=11$. $5147\,{\rm J/g}$ for the B2-B19 transformation and $\Delta H2=11$. $889\,5\,{\rm J/g}$ for the reverse transformation. The second DSC peak appearing at lower temperature is diffuse and the characteristic parameters can not be discerned clearly from the peak.

3.3 X-ray Diffraction

The results of X-ray diffraction at various temperatures confirm the cubic B2-orthorhomic B19-monocluinic B19' two-stage transformation of the Ti49Ni41Cu10 alloy on cooling and its reversibility, as shown in Fig. 4. At 329 K(Fig. 4(a)) the diffraction peak is indentified as the (110) reflection from the B2 parent phase. The lattice parameter of B2 is a_0 (B2) = 0. 3030 nm. At 303 K (Fig. 4(b)) the

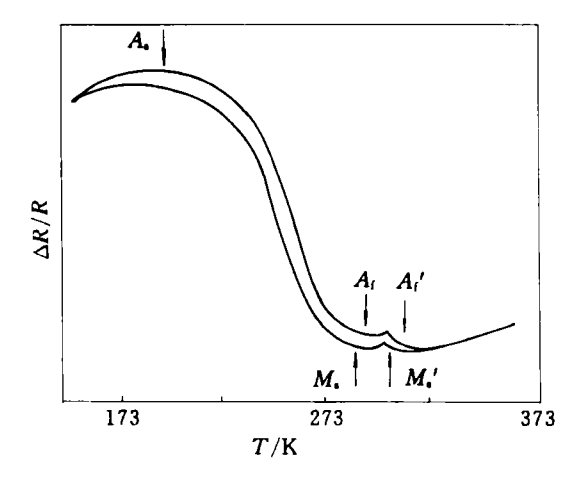


Fig. 2 R-T curve of Ti49Ni41Cu10 alloy

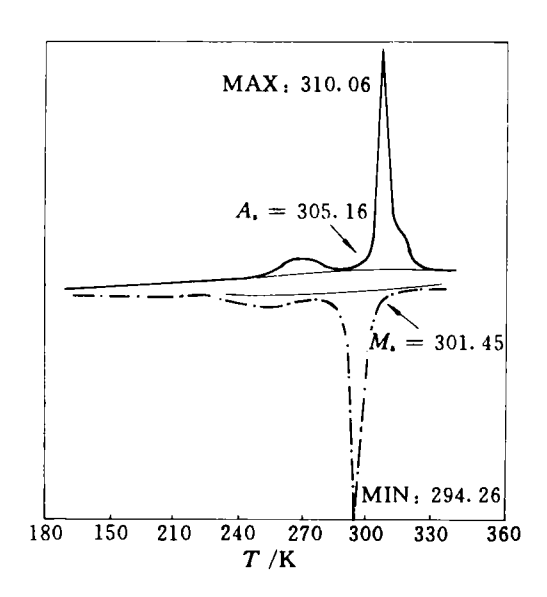


Fig. 3 DSC curve of Ti49Ni41Cu10 alloy

diffraction peaks of the orthorhomic B19: $(110)_0$, $(111)_0$, $(012)_0$, appear coexisting with the (110)_B. This corresponds to the first stage B2-B19 transformation on R-T and DSC curves. The lattice parameters of the B19 martensite are: $a_0(B19) = 0.286 \ 0 \ \text{nm}$, $b_0(B19) = 0.4301 \,\mathrm{nm}, c_0(B19) = 0.4515 \,\mathrm{nm}.$ On further cooling to 287K (Fig. 4(c)) the diffraction peak of monocinic B19' martensite $(111)_{m}$ comes to appear, while $(110)_{0}$, $(020)_{0}$ peaks of the B19 martensite are still obvious. That means the B19-B19' transformation takes place. The lattice parameters of the B19' martensite are: $a_0(B19') = 0.2920 \text{ nm}$, $b_0(B19') = 0.4220 \text{ nm}, c_0(B19') = 0.4602$ nm, $\beta = 96^{\circ}$. With further decreasing temperature the diffraction peaks of the B19' martensite increase and their intensities become strong (Fig. 4 (d-e)). But it is noticed that there exist still peaks of the B19 martensite at 203 K. The fact indicates that the B19-B19' transformation takes place at about 287 K but it is still not complete at 203 K. After heating the specimens again to 333 K, the diffraction profile reverses to that of the B2 parent phase (Fig. 4(f)).

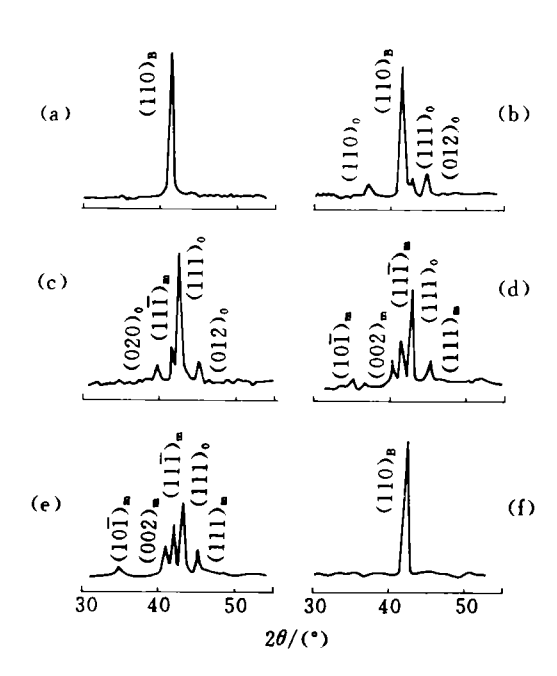


Fig. 4 X-ray diffraction profile at various temperature in Ti49Ni41Cu10 alloy

(a) $-T = 329 \,\mathrm{K}$; (b) $-T = 303 \,\mathrm{K}$; (c) $-T = 287 \,\mathrm{K}$; (d) $-T = 253 \,\mathrm{K}$; (e) $-T = 203 \,\mathrm{K}$; (f) $-T = 333 \,\mathrm{K}$

3.4 TEM Observation

In situ TEM observation on B2-B19 transformation of the Ti49Ni41Cu10 alloy shows that the martensite plates in the early stages have none of stacking fault and twin substructure^[7]. But obvious twins have been observed in the B19' martensite when $T < M_s$, as shown in Fig. 5.

3.5 Elastic Modulus vs Temperature

The elastic modulus variation on cooling has been measured by using flexural resonant-bar technique. The results for the Ti49Ni41Cu10 alloy and Ni51Ti49 alloy are shown in Fig. 6, where f_0 is the resonant frequency and it is proportional to the square root of the elastic modulus $E: f_0 \propto \sqrt{E}$. It is visible from the figure that f_0 of the Ti49Ni41Cu10 alloy abrupt drops with decreasing temperature from 298 K to 293 K. It is well worth notice that this temperature range just corresponds to B2-B19 transforma-

tion. The result indicates an obvious softening of the elastic modulus accompanying the B2-B19 transformation, which is similar to that in binary alloys. From 293 K to 258 K the decrease of $f_{\rm 0}$ value slows down and its value is still in the bottom of the curve. After T < 258 K, $f_{\rm 0} - T$ curve appears raising tendency because of the increasing B19' martensite. The fact implies that the the B19' martensite

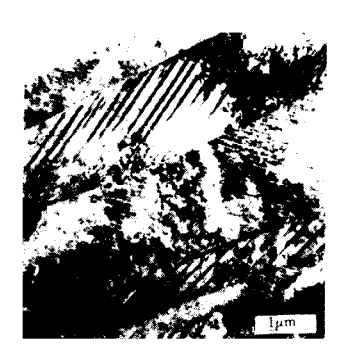


Fig. 5 TEM bright field photography showing twin substructure of B19' martensite

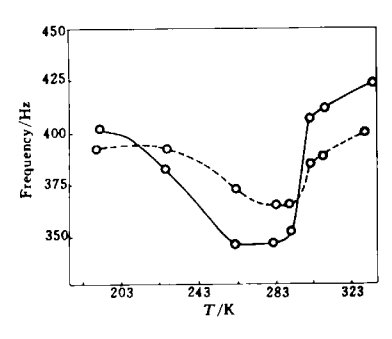


Fig. 6 Resonant frequency elastic modulus

vs temperature curve of Ti49Ni41Cu10

alloy(solid line) and Ni51Ti49

alloy(dotted line)

has higher elastic modulus than B19 marten-

4 DISCUSSION

4. 1 The Characters of Two-stage Transformation

in Ti49Ni41Cu10 Alloy

It is know from above experimental results that the B2-B19-B19' two-stage transformation in the Ti49Ni41Cu10 alloy is temperature-induced and completely reversible. It could be hypothesized that the chemical free energies of the B2, B19 and B19' phases variate with temperature as shown in Fig. 7, where T_0' is the thermodynamical equilibrium temperature between B2 and B19, $\Delta T'$ is the undercooling required by transformation of B2-B19; T_0 and ΔT are that for B19-B19' transformation. Decreasing temperature, as driving force, leads to the successive occurrence of B-B19-B19' transformation.

The B-B19 and B19-B19' transformations exhibit quite different behaviours, especially in the physical properties; the former has a significant transformation heat effect, but a minor resistivity change, while the latter has a small transformation heat effect but an obvious resistivity change, which is 15-20 times large than that of the B2-B19 transformation. Why the opposite behaviour can arise? We guess, it might be related to the difference in martensite lattice type and substructure between B19 and B19'. It is known that electrical

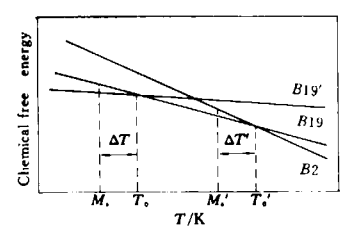


Fig. 7 Schematic of free-energy curves

resistivity is the resistance to the directional moving free-electrons, caused by scattering of irons in the metallic lattice. Generally, the chemical composition, atomic order or disorder in the lattice, dispersion of microstructure and lattice defect can cause the change of lattice periodicity, therefore, influence the resistivity of the alloy. But only the last one (lattice defect) should be the major influencing factor in our discussed situation, because martensitic transformation is a diffusionless transformation. On the other hand, martensitic transformation has the character of an undistorted plane strain. The transformation shear includes two parts: lattice variant homogeneous shear and lattice invariant microunhomogenous shear. The latter leads to stacking fault or twin substructure of the martensite. The TEM experiment has revealed twin substructure of the B19' martensite and defect-free B19 martensite, that agrees with the report in [8][9]. According to the crystallographic phenomenal theory, the principal lattice distortions of cubic B2-orthorhomic B19 transformation are the follows: $\eta 1' = a_0(B19)/a_0(B2) = 0.944, \eta 2' =$ $b_0(B19)/2 \ a_0(B2) = 1.004, \ \eta 3' = c_0(B19)/2$ $a_0(B2) = 1.054$. It is noticed that $\eta 1' < 1$, $\eta 2'$ ≈ 1 , $\eta 3' > 1$. This means, the transformation strain itself satisfies the condition for an undistorted plane and no additional lattice invariant shear is required. But the B19-B19' transformation does not satisfy the condition, therefore twin substructure appears. This deduction conforms to the experimental observation. It is reasonable to suggest that the obvious difference in the resistivity change of the B2-B19 and B19-B19' transformation is due to the different martensite substruction. The transformation heat effect would reflect the energy required by transformation. The transformation form cubic B2 to orthorhomic B19 necessitates large lattice variant homogeneous shear and it must overcome high energy barriers because of the large difference in lattice type and parameters. But the monoclinic distortion with small difference in lattice parameters for B19-B19' is more easy in progress.

That may be the reason for different transformation heat effect between the first and the second transformation.

4. 2 Comparison of Transformation in Ternary Ti49Ni41Cu10 Alloy and Binary Ni51Ti49 Alloy

The ternary and binary alloys both undergo two-stage transformation: B2-B19-B19' for the TiNiCu alloy and B2-R-B19' for the NiTi alloy. The resistivity change with martensitic transformation increases for the ternary alloy and decreases for the binary alloy, as mentioned in section 3. 1. It is noticed that the B2-B19 transformation in ternary alloy and the B2-R transformation in binary alloy both have small transformation hysteresis; the former is about 5K, the latter is $1\sim2$ K. The recoverable strain of B2-R is smaller (<1%), that gives a restriction for its application. However, the recoverable strain of B2-B19 transformation is larger^[10], that shows a wide use prospects.

It has been found from elastic modulus measurement that the martensitic transformation in ternary alloy is accompanied with a pronounced softening of E modulus, which is similar to the transformation described by soft modes in binary alloy. The fact implies the similitude of transformation nature in both alloys.

5 CONCLUSIONS

- (1) The martensitic transformation of a Ti49Ni41Cu10 alloy undergoes two-stage transformation: cubic B2-orthorhomic B19-monoclinic B19'. The transformation is completely reversible.
- (2) The characters of the B2-B19 transformation are; significant transformation heat effect, small resistivity change, narrow transformation temperature range with about 5 K temperature hysteresis and pronounced softening of E modulus. The B19 martensite has none of stacking fault and twin substructure.

(To page 75)

- 5th ICSMA, Pergamon Press, 1979.
- 2 Peters, M; Gysler, A; Lutjering, G. AIME, 1980, 1777.
- 3 Stubbington, C A; Bowen, A W. J Mater Sci, 1974, 9: 941.
- 4 Peters, M. Lutjering, G. AIME, 1980, 925.
- 5 Peters, M; Lutjering, G. EPRI CS-2933, 1983.
- 6 Zhang, S Q; Tao, C H; Yan, M G. ASTM STP942, 1988, 838.
- 7 Tao, C H; Zhang, S Q. In: Proc 5th Inter Conf Mech Behavior of Materials, Beijing, 1987.
- 8 Zhang, S Q. Acta Metallurgica Sinica, 1983, 19A (6): 551.
- Welsch, G; Lutjering, G; Gazioglu, K; Bunk,
 W. Met Trans 1977, 8A; 169.
- 10 Blackburn, M A. Metall Soc AIME, 1967, 239, 1200.

- 11 Rosenberg, H W. The Science, Technology and Application of Titanium. London: Pergamon Press, 1970. 851.
- 12 Margolin, H; Williams, J C; Chesnutt J C; Lutjering, G. In: Proc 4th Inter Conf on Titanium, Kyoto, Japan, 1980.
- Williams J C; Lutering, G. In: Proc 4th Inter Conf on Tianium, Kyotot, Japan, 1980.
- 14 Blackburn, M J; Williams, J C. Trans ASM 1969, 62: 398.
- 15 Lutjering, G; Weissmann, S. Acta Met, 1970, 18: 185.
- 16 Hamajima, T; Lutjering, G; Gerold, V. Acta Met, 1974, 22: 901.
- 17 Tao, C H; Zhang, S Q. J of Aero Mater, 1989, 9(2): 32.

(From page 65)

(3) The characters of the B19-B19' transformation are: obvious resistivity change, minor heat effect and wide transformation temperature range. B19 martensite has higher E modulus than the B19 martensite and has twin substructure.

REFERENCES

- 1 Zhang, Y; Hornbogen, E Z. Metallkde, 1987, 78 (H6): 401.
- 2 Bricknell, R H; Melton, K N; Mercier, O. Met Trans, 1979, 10A; 693.
- 3 Miyazaki, S; Shioto, I; Otsuka, K; Tamura, H. MRS Int Mtg Adv Mates, 1988, 9; 153.

- 4 Saburi, T; Nenno, S. In: Shanghai Iron and Steel Research Institute(ed), The Proce of The 3rd China-Japan Metal Physics and Physical Metallurgy Symposium, Shanghai: 1988: 61.
- Jin, J L; Zhang, Y; Cai, X X. In: The Proce of the SMM-94 Int Symposium, Beijing: 1994.
- 6 Miyazaki, S; Wayman, C M. Acta Metall, 1988, 36(1): 181.
- 7 Zhang, Y; Ji, Z Q; Gai, G Q. Technical Report of SISRI, 1993, (6): 8.
- Tadaki, T; Wayman, C M. Metallography, 1982, 15: 233, 247.
- Saburi, T; KOmatsu, T; Nenno, S; Watanabe,
 Y. J of Less-Common Metals. 1986, 118: 217.
- 10 Nam, T H; Saburi, T; Kawamura, Y; Shimizu, K. Materials Trans JIM, 1990, 31: 262.